Different Design Aspects Of Swirl Jet Using Vortex Generating Jets

سمات تصميمية مختلفة في النفث الحلزوني باستعمال النفاثات المولده للدوامات

by

N. H. Mostafa and **U. Vandsburger**
Visiting Prof. **Assist. Professor**
Mechanical Engineering
VIRGINIA POLYTECHNIC INSTITUTE AND STATE UNIVERSITY

خلاصة:-

تمت عمليادراسه خطوط المسار لدوامه أنتجت من تأثير نفث دائرى مع نفاثات سطحية وتأثيرذلك على إضطراب الطبقات المتلخمة.

ان النفاثات السطحية استعملت كمولدات للنفث الحلزونى وذلك للتحكم فى النفث الرئيسى. هذه النفاثات السطحية قد حقنت بزوايا ميل قدرها صفر ، ٩٠،٤٥ درجة فى الإتجاه المماسى للنفث الرئيسى مما احدث زيادة فى معدل نمو النفث الرئيسي بمقدار ٥ و١٠ و ٨ درجات على التتابع. وقد وجد انه فى حاله الحقن المماسى ينقسم النفث الرئيسى الى اربعه دوامات متعاكسه الاتجاه بينما فى حاله الحقن بزاويه ٤٥ درجه تحدث مجموعه منتشره من الدوامات. و كذلك فان منحنى السرعه القطريه يحقق اعلى قيم فى الحقن بزاويه ٤٥ درجه. و على العكس فان منحنى السرعه الحلازونيه يحقق اعلى قيم فى الحقن المماسى حتى مسافه رأسيه تساوى عشره اضعاف قطر المنفث. أن نسبة سرعة النفاثات السطحية الىسرعه النفث الرئيسى تساوى من ٨, الى ١،٢. و بمقارنة الحالات المختلفة ظهر ان الدوامات المنتجة فى النفث الرئيسى تم التحكم التام فيها بواسطة تغيير زاوية حقن وكثافة و اسلوب توزيع النفث بالنفاثات السطحيه .

ان تحليل الصور اعطى معلومات عن طبيعة السريان خلال النفث الحلزونى. كما ان مشاهدة المائع قد أعطت نتائج قويه الإرتباط مع نتائج قياس السرعات .

Abstract

Longitudinal streamwise vortices produced by the interaction of simple round jets with peripheral jets affecting turbulent boundary layer were investigated experimentally. The peripheral jets are used as Swirl Generator Jets (SGJ) for controlling the main jet. These jets (SGJ) were pitched up with injection inclination angle of zero , 45 and 90 degrees to the tangent direction of the main jet. The ratio of peripheral jet velocity to the free main jet velocity ($VR = C_i / C_m$) is considered in the range of 0.8 to 1.2. The comparison of different conditions showed that the vortices produced in the jets are completely controlled by SGJs injection angle and intensity. Increasing the injection angle was found to increase the growth rate of the main jet .

Image analysis also gave average spatial information about the mass entrainment through the swirl jet. Results of flow visualizations and quantitative measurements are strongly resemble each other.

Nomenclature

C: Absolute velocity (m/s).
C_m: Velocity of main jet (m/s).
C_j : Velocity of peripheral jet (m/s).
d : Diameter of peripheral nozzle (mm).
D : Diameter of main jet (mm).
L : Axial distance from nozzle exit (mm)
U : Axial velocity (m/s).
r, t : Local polar radial and tangential coordinates.
V : Velocity in X-direction (m/s).
V_R : Radial velocity relative to local radial axis (+ ve value for outward direction) (m/s).
VR : Ratio of the peripheral jet velocity to the main jet velocity (without injection).
W : Normal velocity component in z direction (m/s).
W_t : Swirl velocity relative to local tangent axis(+ve value for anti-clockwise direction) (m/s).
y : Axial coordinate.
x, z :Coordinates along and normal to the horizontal surface.
α : injection inclination angle (angle between the peripheral jet axis and the tangent surface of the main jet, or the wind tunnel, in the horizontal plane) (degrees).
β : jet azimuthal angle (angle between the jet axis and the wind tunnel free-stream direction) (degrees).
ϑ : Divergent growth flow angle, measured between jet sides (degrees).

Introduction

Relative performance of several passive and active methods for controlling two dimensional turbulent separated flow is associated with vorticity generating behavior. Vortex generators have long been known to increase the mixing (through direct injection) between external streams and boundary layers. [1]

Lin and et al., [2] varied the jet orientation through the horizontal surface of wind tunnel. The authors changed the jet inclination angle (α) and the jet azimuthal angle (β). The Vortex Generator Jets (VGJ) were effective in reducing separation. VGJ's seem to perform best for azimuth angles (β) of 90° to 30° and for inclination angles (α) of 15° to 25°. There was no effect on separation for VGJ's blowing vertically (α =90°) . The highest velocity ratio was the most effective in separation control.

Induced jets of wind tunnel flow are closely similar to conventional vortex generators. But, vortex inside jets generated using vortex ring [3], small tabs at the nozzle exit [4] or crown-shaped nozzles [5] are passive control methods. Active control of mixing in jets is achieved by sound wave or perturbation of jet wall [6]. These method have many problems like increasing environmental noise intensity. Also, the perturbed material (Piezoelectric) works at low temperature only (40° degrees).

The principal objective of the present research is to investigate the relative performance of several swirl jet design aspects for active and passive control of jet turbulent boundary layer mixing. This may be done by optimization of the inclination angle of peripheral jets injected into the main jet. The active flow control mechanism for swirl jets is applied by varying velocity ratios (injection velocity to main free stream velocity). The flow visualization techniques will be used in order to describe and confirm the flow mechanism. Quantitative 3-D velocities are measured for complete understanding of the phenomenon.

Experimental Facility and Methods

A swirl jet of 13 mm diameter and four peripheral jets (2 mm Id) are manufactured at the reacting flows laboratory of the mechanical engineering department in Virginia Polytechnic Institute. Three different jets were used for different inclination angles of peripheral jets (0°, 45° and 90°). To measure the swirl jet flow mechanism, a combination of flow visualization, image processing techniques and quantitative 3-D velocity measurement is used.

A seven hole probe is used to measure 3-D velocities of jet at vertical plane. This trapezoidal vertical plane is traversed parallel to the jet centerline up to 43 mm away from the diametric plane. Figure (1) demonstrates the measured zone in these planes.

The flow visualization experiments were carried out using a laser sheet. A 4-w argon-ion laser at 514.5 nanometer, wave length, was used as the light source. Appropriate lenses were used to form a laser sheet of approximately 1 mm thickness to view the desired cross section of the jet.

Elastic light scattering from mineral oil smoke particles which were introduced into the main jet fluid was employed for flow visualization. The scattered light was collected by a Cohu model 6410 CCD array camera with 739 X 484 active picture elements and a pickup area of 6.4 X 4.7 mm. The images were then grabbed and stored by a PC-486 as demonstrated in Fig (2).

The Image resolution was 512 X 480 pixels, which corresponded to an imaged area of approximately 80 mm X 60 mm. Various cross-sections through the jet, both vertical and horizontal, were imaged. Image processing was also done on a PC-486 using Image Proplus 2.0 soft ware. After correction, the pixels in each image were binded to create 8 X 8 "super pixels", each representing a probe volume of approximately 1 mm^3. The binding was performed to increase the signal to noise ratio, at the expense of spatial resolution. The date was then used to create two-and three-dimensional iso-concentration plots using Tecplot 6.0 software.

Results

Flow visualization was performed in non-reacting flows to examine the effects of variation of the injection angle (α) and velocity ratio (VR) on the swirl jet . Flow velocities were measured to shed further light on the flow mechanism.

Figure (3) shows vertical pictures of the swirl jets taken by radial vertical laser sheet. It demonstrates iso-light intensity reflected from the smoke particles laden with jet flow. These contours represent streamwise jet. The contour line with light ratio 0.9 represents the flow of the jet core. The height of these particular pictures was taken up to eight times of the jet diameter. Main jet exit velocity was 17 m/s. The first picture (Fig. 3.a) is the reference case of the jet without generating swirl. In the three other pictures (Figures 3.b, 3.c, 3.d), the injection inclination angle changes from zero (tangent injection) to 45 and 90 degrees (radial injection). A comparison of these views reveals the great effect of swirl on the jet flow growth angle. The streamline grows faster in tangent swirl jet by about five degrees. Furthermore, the 45 and 90 degrees injection conditions increase the divergent angle by 10 and 8 degrees, respectively, compared with normal jet conditions. This means that, the maximum growth flow angle is achieved at injection angle 45 degrees.

To confirm these trajectories quantitative measurements were taken with a seven hole probe. These 3D-velocities are measured at an axisymmetric vertical trapezoidal sheet divided into 1260 nodes as the measuring locations. Figure (4) compares the iso-axial velocity line in the radial vertical sheet for injection angles zero and 45°. These contour lines give approximately the same results of the visualization technique. For certainty, the divergent growth flow angle of swirl jet conditions calculated from the iso-axial velocity lines is lower by about two degrees than that determined by visualization techniques. This difference is due to the laser sheet picture representing the stream line of the absolute velocity, while the velocity contour lines represent the axial velocity. The response surface of axial velocity along the radial vertical sheet gives a complete view of this distribution. It is clear that the axial velocity has a larger radial distribution, at jet down stream, for 45 degrees injection angle conditions.

Evolution of axisymmetric jets perturbed by peripheral jets with different injection angles are introduced by laser sheet cross section in Fig.(5). The laser intensity displays only the deviation of the main jet flow mechanism. This is due to the smoke which is only generated in the main flow. The contours of iso-light intensity indicates the form of the flow mechanism. The maximum and the minimum deflections of these contours are at 45° and 90° conditions respectively (compared to normal condition). There are many corrugated lines related to eddies at the outer surface in the tangent condition.

Figure(6) shows two sets of 3-D mean streamwise velocities in horizontal plane of jet exit for zero and 45° degrees injection angles. The iso-axial velocity contours, look qualitatively very similar to the laser-illuminated images, as in Fig.(5). The resultant vectors of swirl and radial velocities (Wt & Vr) are plotted relative to its directions and magnitudes at each point. The vortices generated in the tangent injection conditions are in opposite directions to each other, but, the vortices generated by the 45 degree injection jets are more disturbed with some little eddies.

Figure (7) shows the velocity profiles for each of the axial, radial and normal velocities along the radial direction at 0.01 mm and 14 mm from the jet exit. It is clear that the swirl peak velocity profile diffused from around the jet surface (at its exit) to the outside and core of the jet (at 14 mm from jet exit).

Three pictures sets (Fig. 8) have different vertical levels up to L/D equals five. All these pictures are represented by iso-light intensity ratio ranged from 0.2 to 0.86 with step equals 0.22. One can see that, the 45 degree injection gives maximum flow deviation up to 5 L/D. On the other hand, the tangent and 90 degree injections are affected up to 4 L/D.

By following the radial velocity along the vertical radial plane, the response surface will be obtained as shown in Fig. (9). The radial velocity profiles are almost similar to the three dimensional surface between 0 and 45 degrees injection conditions, but maximum peak value are much higher at 45 degrees injection angle conditions. The radial velocity has its peak value at jet core which can be observed from the iso-contour lines.

The normal velocity profiles along the radial vertical sheet, as iso-contour lines and response surface, for zero and 45 degree injection angles are compared in Fig.(10). At down stream up to L/D equals ten, the tangent injection angle conditions have higher amplitude than the 45 degree injection angle conditions. When moving farther down stream, swirl distribution becomes higher at 45 degree injection angle.

Figure(11) compares the iso-laser pixel values (or entrained mass of smoke) along the geometric horizontal cross section (at L/D equals one) of each picture. One can see that the peripheral jet to main jet velocity ratio ($C_j/C=1.2$) tends to move the core flow inside along the vertical axis with higher deviations than at lower velocity ratio ($C_j/C=0.8$). Both cases have the same flow rate into the main jet. Figure (11.c) shows that the deviation from one jet is more than the others. Finally, these cases demonstrate the methods of active jet control (jet geometry control) by changing velocity ratio or injecting one peripheral jet more or less than the others.

Conclusion

This study of the effects of the peripheral jet (orientation and speed) on streamwise vortices of the swirl jet shows that the use of peripheral jets provide direct control of the swirl jet characteristics.

The peripheral jets configurations indicate the shape of the jet streamwise spreading and almost any arbitrary shape can be obtained by the proper placement of the peripheral jets.

Flow visualization and mean velocity measurements present consistent images of the swirl jet patterns.

Jet flow streamwise indicates that the divergent flow angle increases by about 5°, 10° ,or 8° (from the normal jet) by increasing injection angle from 0 to 45 to 90 degrees respectively.

The vortex generated in the horizontal plane from the peripheral jets is a function of the injection angle. In tangent condition four vortices are generated in opposite direction to each other, but the vortices generated by the 45 degree injection angle are more disturbed and divided to eddies.

In the 45 degree injection angle the radial velocity profile along the radial vertical sheet has a higher maximum value than with tangent injection condition.

The swirl velocity profile and eddies at the jet surface have higher magnitude in case of tangent peripheral jets up to L/D equal ten. Moving farther down stream swirl distributions become higher at 45 degree injection angle.

Active control of jet geometry can be achieved easily by controlling the velocity ratio as well as by injection one peripheral jet more or less than the others.

Acknowledgments

The authors wish to thank Eng. S. Marcous (Ph. D. student) for his assistance in the combustion lab.

References

1. Johnston, J. P. and Nishi, M. "Vortex Generator Jets-Means for Flow Separation Control" AIAA Journal, Vol. 28, No. 6, pp. 989-994, June 1990.
2. Lin, L.C., Howard, F. G., Bushnel, D. M. and Selby, G. V. "Investigation of Several Passive and Active Methods for Turbulent Flow Separation Control" AIAA 21st Fluid Dynamics, Plasma Dynamics and Lasers Conference. Seattle, WA. AIAA 90 1598. June 18-20, 1990.
3. Yamasaki, H., Kitazawa, S. and Zhang, Z. M. "Forming 2-Dimensional Jet Flow by Vortex Ring in Fluidic Devices" FLUCOME 91, pp. 291, ASME 1991.
4. Samimy, M., Zaman, K. B. M. Q. and Reeder, M. F. "Effect of Tabs on the Flow and Noise Field of an Axisymmetric Jet" AIAA journal, Vol., 31, No., PP 609-619, April 1993.
5. Zaman, K. B. M. Q. and Reader, M. F and Samimy, M. "Control of an Axisymmetric Jet Vortex Generators" J. Phys. Fluid Vol. 6, No. 2, PP. 778-793, February 1994.
6. Grinstein, F. F. and Gutmark, E., Parr T., and Hanson-Parr, D. "Computational and Experimental Study of Controlled Mixing in a Circular Jet" 15th. AIAA Aeroacoustics Conference/ log Beach, CA., AIAA-93-4364, October 25-27, 1993.

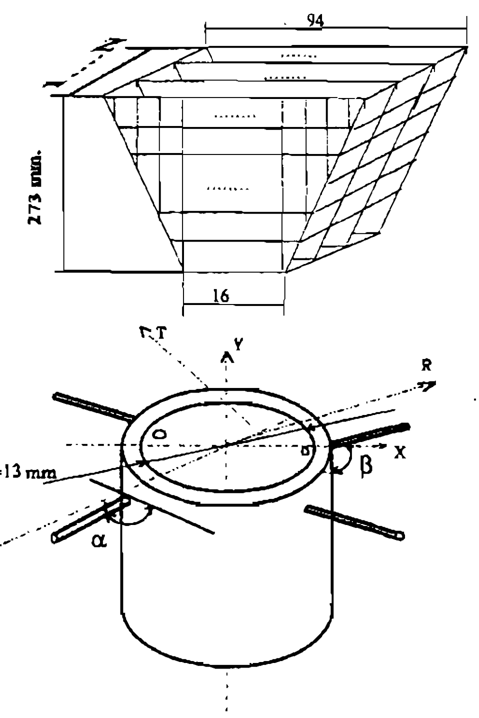

Fig. (1) 3-D Swirl jet construction

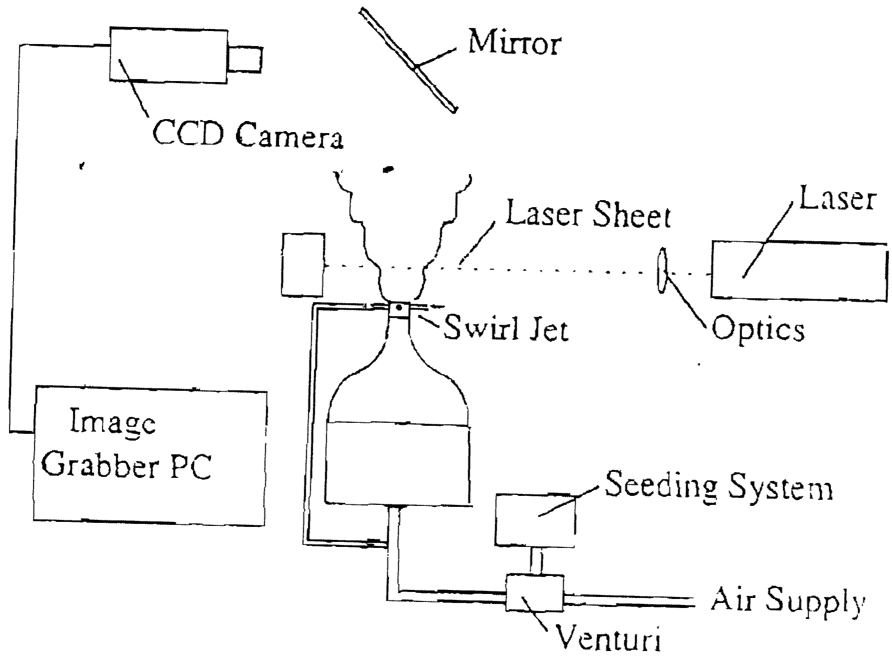

Fig. (2) Laser visualization system and imaging analysis in 2-D.

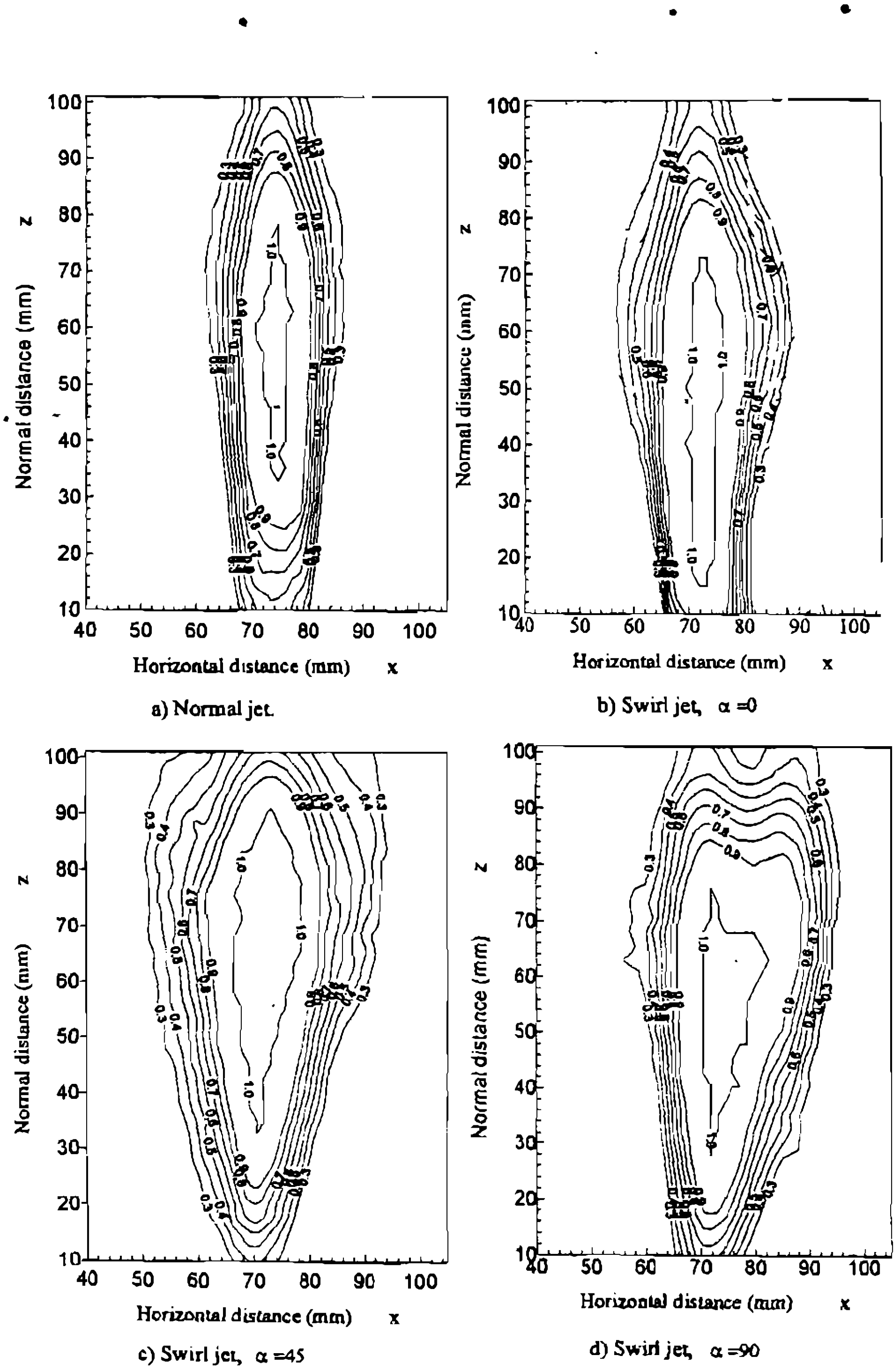

Fig. (3) Reflected laser intensity in vertical diametric plane for different jet conditions.

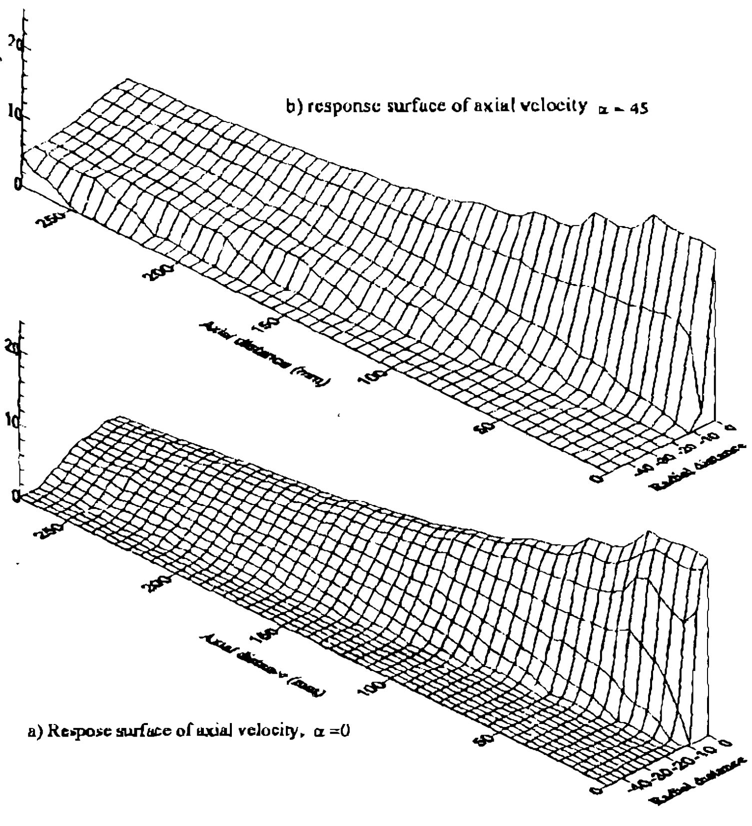

Fig. (4) Axial velocity component in vertical diametric plane of swirl jet.
(half jet view and injection angles 0 &45)

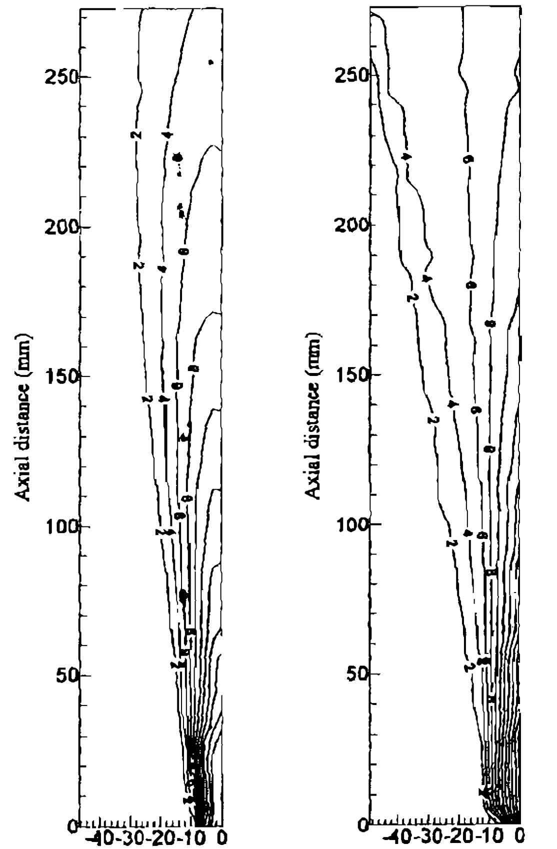

Radial distance (mm)

c) Iso-axial velocity line, α =0

d) Iso-axial velocity line, α =45

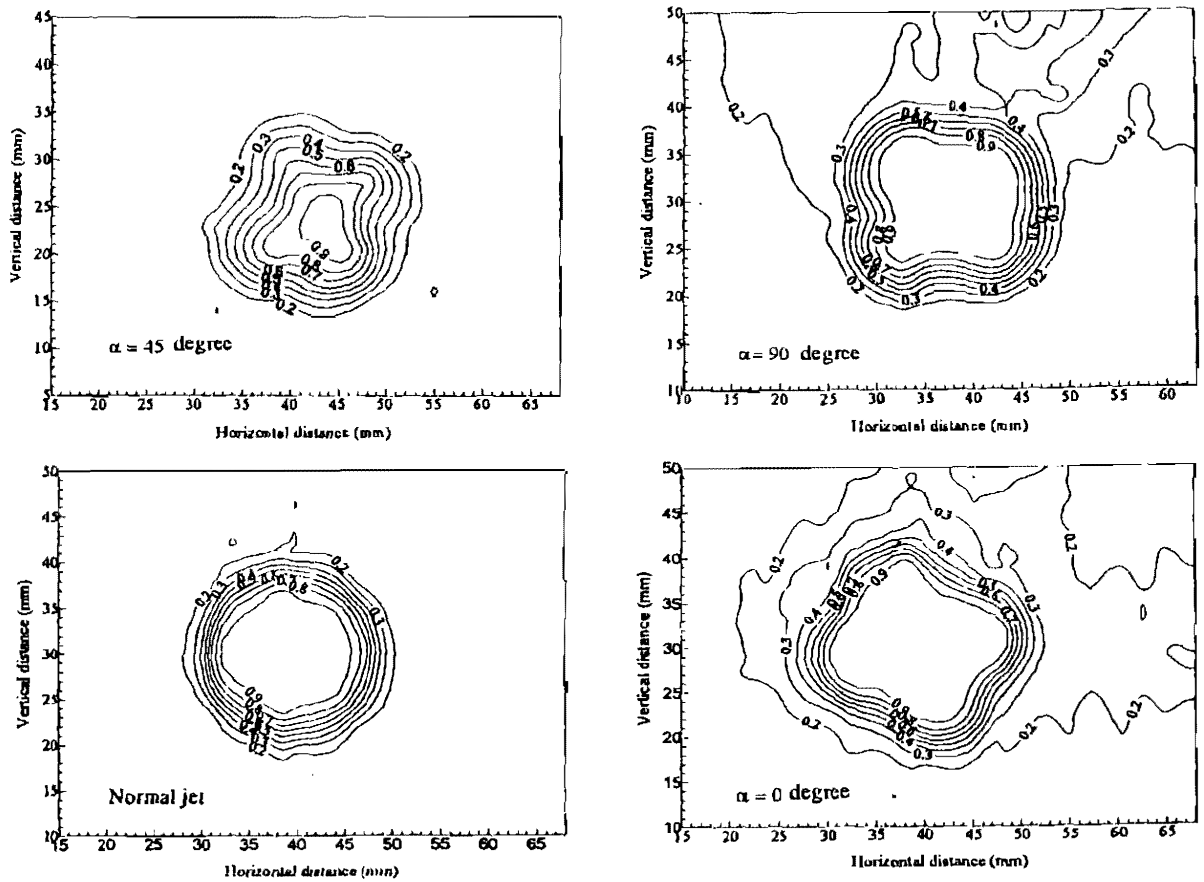

Fig. (5) Horizontal cross section of the main jet by laser sheet, (L/D=1 & Cj/C=1).

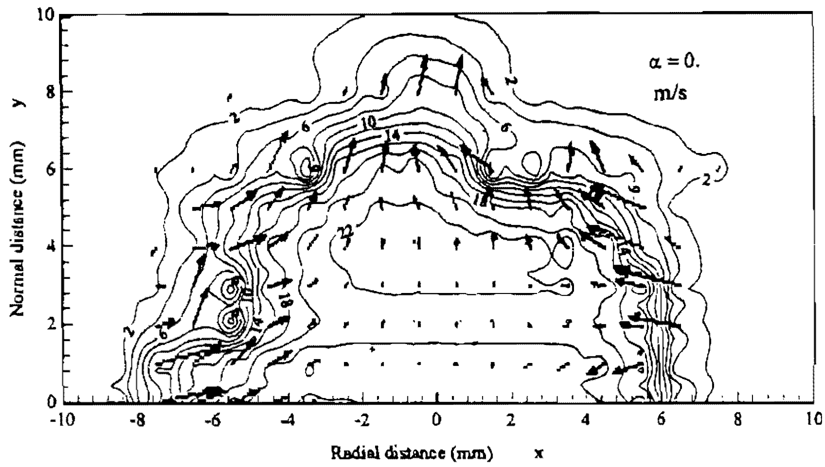

a) Iso-axial velocity lines (m/s) & resultant vector of radial and tangential velocity at jet exit for α = 0.

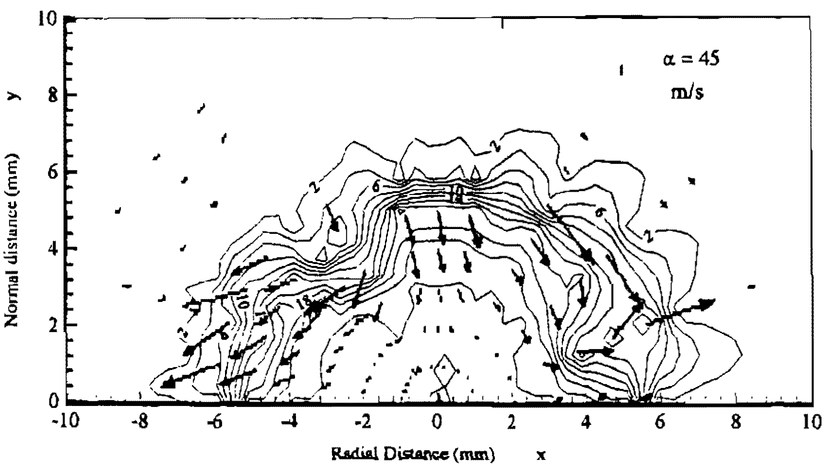

b) Iso-axial velocity lines (m/s) & resultant vector of radial and tangential velocity at jet exit for α = 45.

Fig. (6) 3-D velocity components at horizontal section for swirl jet exit. (half jet at exit, VR=1 and injection angle 0&45 degrees).

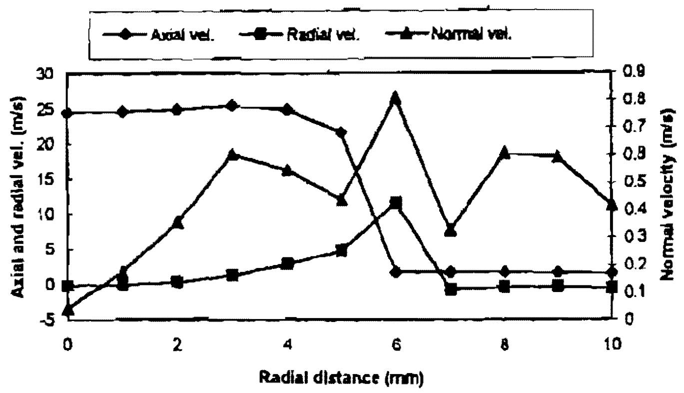

Fig. (7-a) 3-D velocity component at swirl jet exit, (α=45).

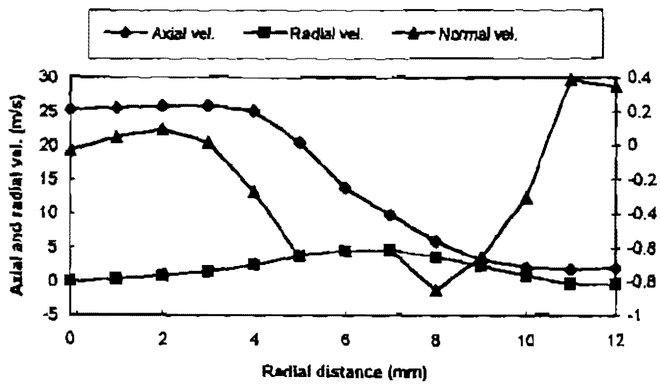

Fig. (7-b) 3-D velocity component of swirl jet (L=14 mm & α=45)

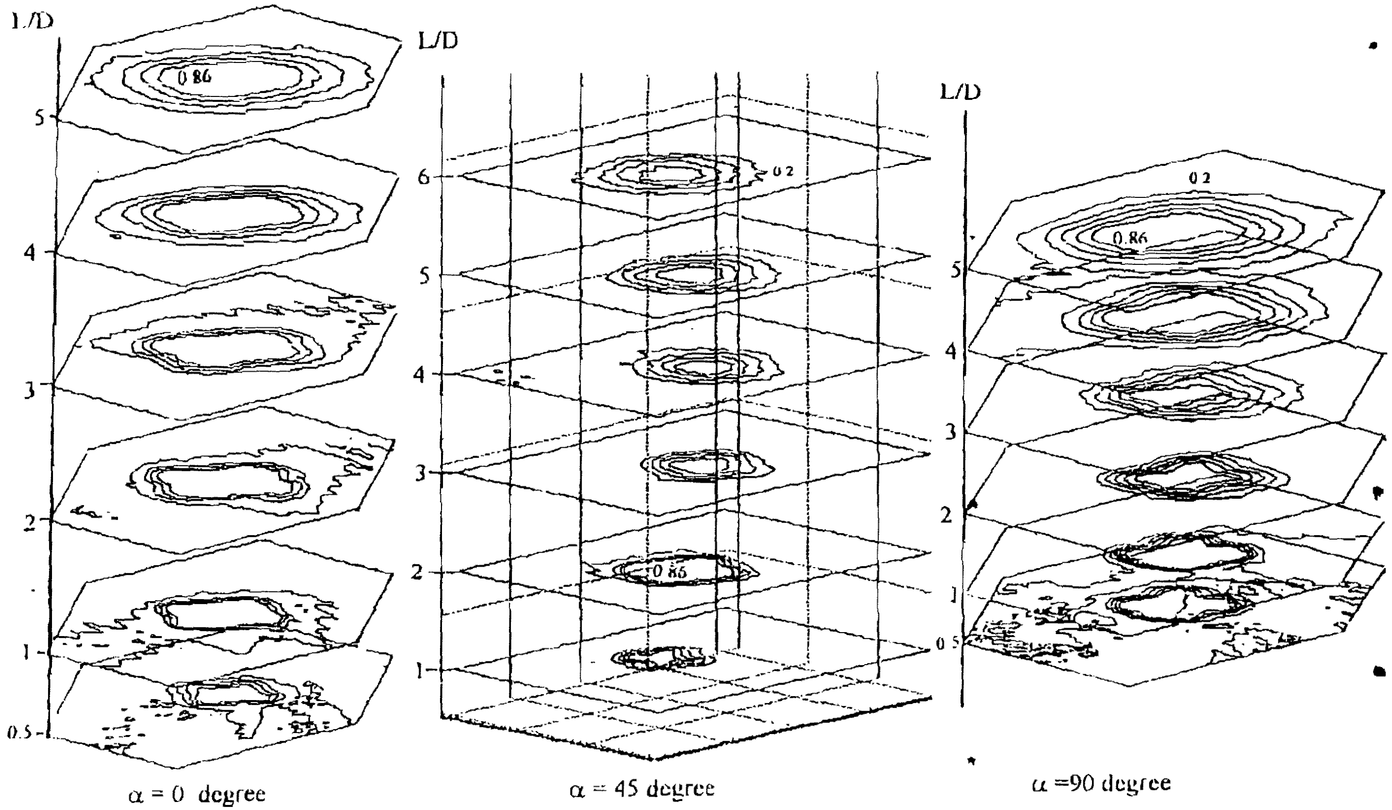

Fig. (8) Multi contour levels by laser sheet up to L/d=5, (Cj/c=1)

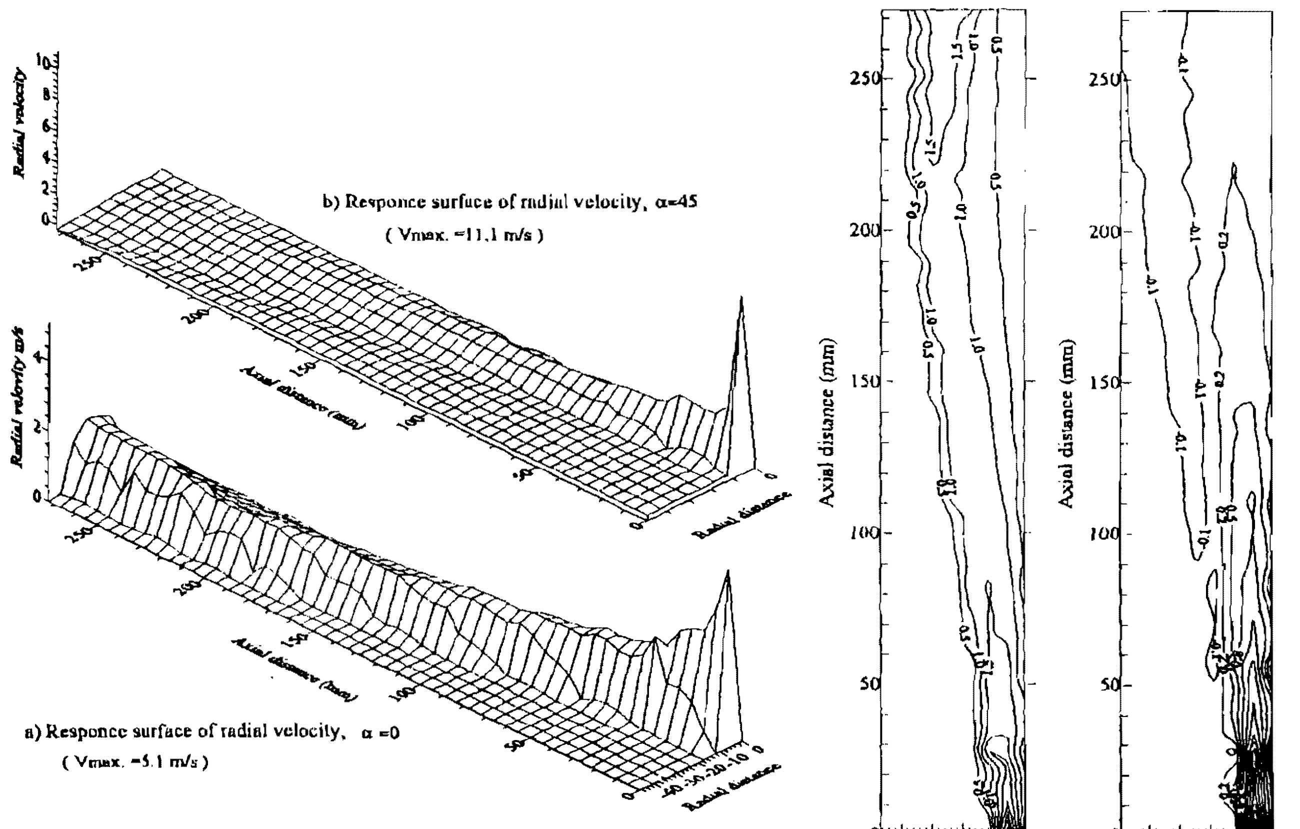

Fig. (9) The radial velocity component in vertical diametric plane of swirl jet.
(half jet view and injection angles 0&45).

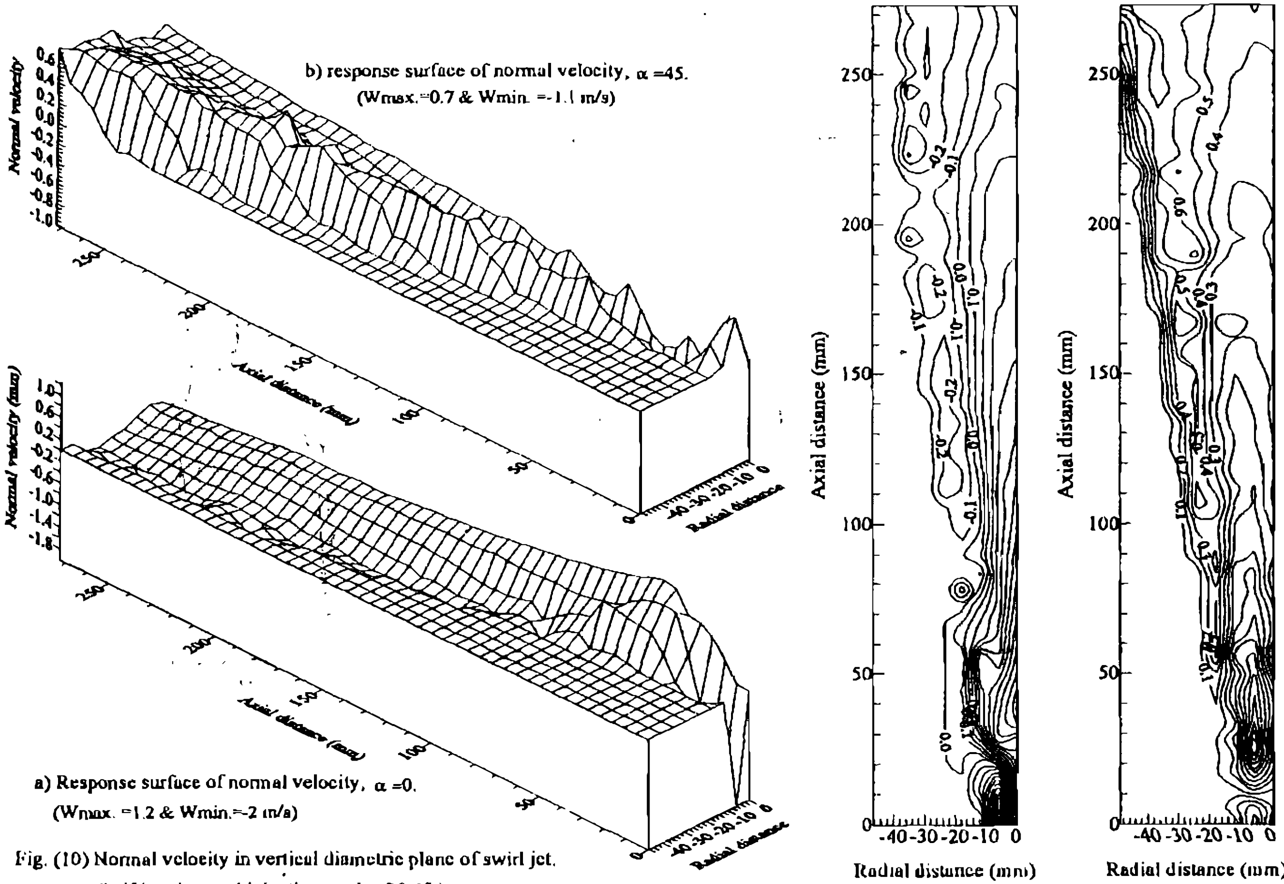

Fig. (10) Normal velocity in vertical diametric plane of swirl jet.
(half jet view and injection angles 0&45)

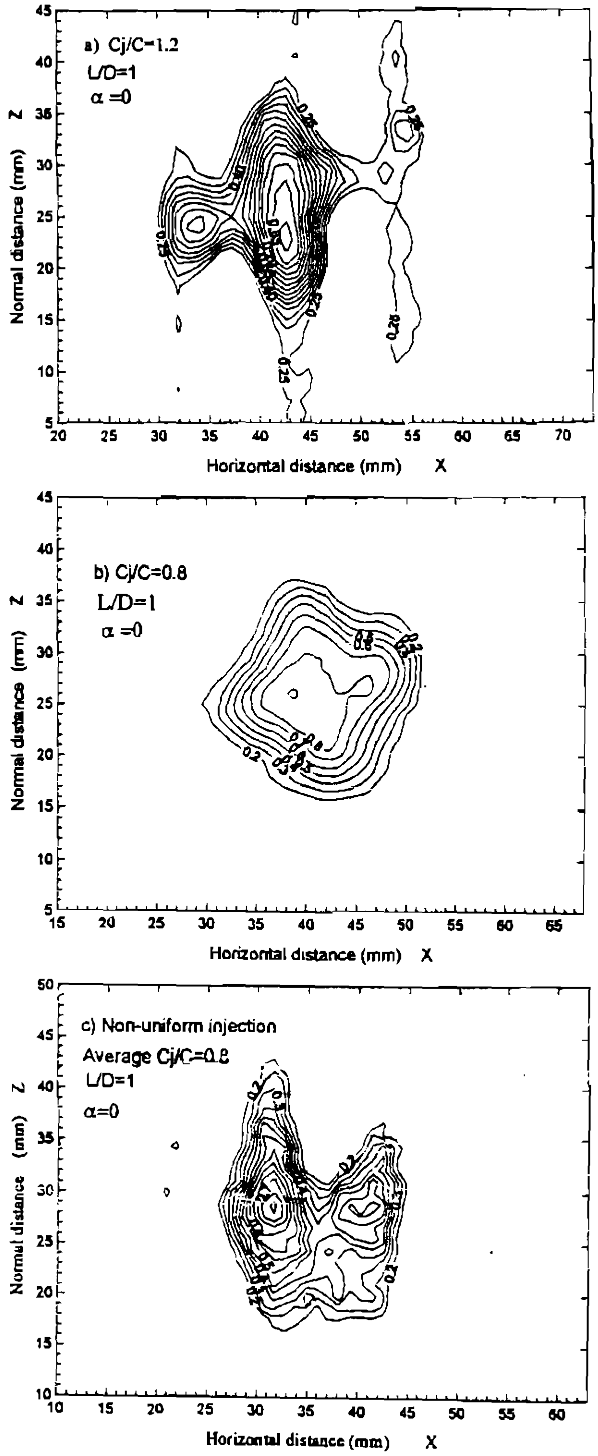

Fig. (11) Reflected laser intensity from swirl jet section at different velocity ratios.